Level crossing methodology applied to line-edge roughness characterization

Chris A. Mack[a], Timothy A. Brunner[b], Xuemei Chen[c], Lei Sun[d],
[a]Fractilia, 1605 Watchhill Rd, Austin, TX 78703
[b]GLOBALFOUNDRIES, Hopewell Junction, NY 12533, [c]GLOBALFOUNDRIES, Malta, NY
[d]GLOBALFOUNDRIES, Albany, NY

Abstract

Stochastic-induced roughness of lithographic features continues to be of great concern due to its impact on semiconductor devices. In particular, rare events (large deviations in edge positions due to roughness) can cause catastrophic failure of a chip, but are hard to predict. Here, a new methodology, the level crossing method, is used to characterize the statistical behavior of edge roughness with the goal of predicting extreme events. Using experimental results from EUV lithography, the distribution of edge deviations was found to have tails significantly heavier than a normal distribution. While further work is required, these heavy tails could prove problematic when EUV is used in high volume manufacturing.

Subject Terms: line-edge roughness, linewidth roughness, stochastic-induced roughness, LER, LWR, level crossing

1. Introduction

The impact of stochastic-induced roughness on lithographic features continues to be of great concern, especially in the realm of EUV lithography. Shrinking feature sizes driven by Moore's Law would ideally be accompanied by proportionally shrinking roughness as well. However, over the last 15 years, as stochastic-induced roughness has gained the attention of the industry, roughness has shrunk at a much slower pace that the mean feature sizes being patterned. As a result, 3σ linewidth roughness now regularly exceeds 10% of the feature size, and is often as high as 25% of the feature size.

There are at least four ways in which stochastic-induced roughness can impact devices made from lithographically defined features:

- Within-feature roughness, affecting the electric or physical performance of the feature
- Feature-to-feature mean critical dimension (CD) variation (also called local CD uniformity, LCDU)
- Feature-to-feature mean pattern placement error
- Rare events that lead to catastrophic failure (such as bridges or breaks)

Ideally, an understanding of the stochastic-induced roughness behavior of a lithographic process would lead to the ability to predict all four of these consequences. Progress has been made in understanding the impact of roughness on the first three items from this list,[1,2] and more attention is now being paid to the last item: catastrophic failures.[3]

In this paper, we introduce a new methodology for characterizing the statistical behavior of stochastic-induced roughness called the level crossing method. It is hoped that this method will contribute to the characterization and understanding of stochastic-induced roughness in general, and the prediction of rare events (catastrophic failures) in particular.

2. Level Crossing for a Stochastic Process

The level crossing problem is a standard one in stochastic time series analysis. First developed by Rice,[4] this problem begins by defining as a random variable the number of times a series crosses the level a over a series length L (Figure 1). We shall ask, what is the expected number of level crossings given a knowledge of the statistical behavior of the rough feature? Note that for large L the number of excursions will be half of the number of level crossings.
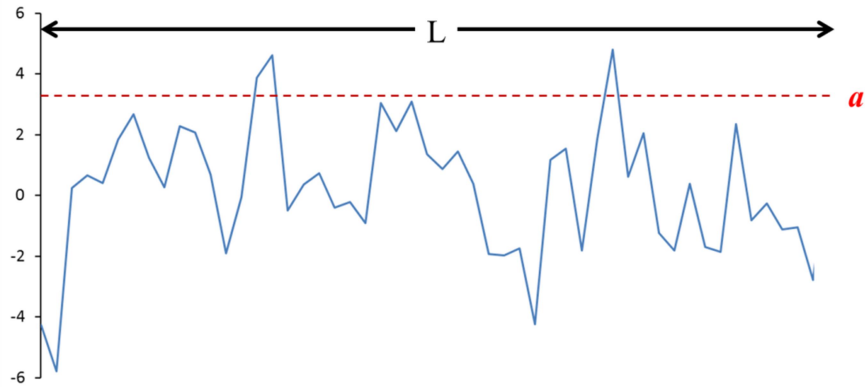

Figure 1. Example of a random stochastic series (such as a rough edge position or linewidth) showing four crossings (two excursions) of the level a within a series of length L.

We define the statistical behavior of the rough feature using a model of the power spectral density (PSD). For example, most LER/LWR data have been found to be well described by the Palasantzas power spectral density function:[5]

$$PSD(f) = \frac{PSD(0)}{\left[1 + \left(2\pi f\xi\right)^2\right]^{H+1/2}} \tag{1}$$

where σ^2 is the true variance of the line edge/linewidth, ξ is the correlation length, H is the Hurst roughness exponent, and PSD(0) is calculated (using the gamma function, Γ) by

$$PSD(0) = 2\sigma^2\xi\left(\frac{\sqrt{\pi}\,\Gamma\left(H + \frac{1}{2}\right)}{\Gamma(H)}\right) \approx (2H+1)\sigma^2\xi \tag{2}$$

The PSD is the Fourier transform of the autocovariance function (ACF) of the rough feature. When $H = 0.5$, the Palasantzas PSD is the Fourier transform of the exponential ACF.

$$ACF(\tau) = \sigma^2 e^{-|\tau|/\xi} \tag{3}$$

For the discrete case, where the stochastic series only exists at discrete intervals spaced Δy apart, this exponential autocovariance model is known as the autoregressive model of order 1, AR(1):

$$ACF(\tau = n\Delta y) = \sigma^2 \rho^n, \quad \rho = e^{-\Delta y / \xi}, \quad n \geq 0 \tag{4}$$

One more statistical behavior must be defined to fully characterize a rough feature: the probability distribution of edge positions/linewidths. Here, we will assume a Gaussian distribution with zero mean and standard deviation σ (the same parameter used in the PSD and ACF models above). The validity of this assumption will prove to have important consequences to our final predictions of rare events, and will be discussed at some length below.

For the case of the discrete AR(1) model and a Gaussian probability distribution, the expected number of zero crossings ($a = 0$) has been previously derived.[6,7] If η_0 is the expectation value of the number of zero crossings, then

$$\rho = \cos\left(\frac{\pi \eta_0}{N-1}\right) \tag{5}$$

where N is the number of points in the series (so that the feature length $L = N\Delta y$). For the case of $\Delta y \ll \xi$, so that ρ is near 1, the inverse cosine can be approximated to give

$$\eta_0 = \frac{N-1}{\pi}\cos^{-1}(\rho) \approx \frac{N-1}{\pi}\sqrt{\frac{2\Delta y}{\xi}}\left(1 - \frac{\Delta y}{6\xi} + O\left(\frac{\Delta y}{\xi}\right)^2\right) \tag{6}$$

Assuming N is sufficiently large, an equivalent approximate expression is

$$\eta_0 \approx \frac{L}{\pi}\sqrt{\frac{2}{\Delta y \xi}} \quad \text{or} \quad \frac{L}{\eta_0} \approx \pi\sqrt{\frac{\Delta y \xi}{2}} \tag{7}$$

The number of zero crossings per unit length is inversely proportional to the square root of the correlation length, and inversely proportional to the square root of the discrete sampling distance, Δy. In other words, the scale parameter for this statistic is $\sqrt{\Delta y \xi}$. The variance of this expected number of zero crossings is $N/4$.

It is common to derive a continuous model from a discrete model by letting $\Delta y \to 0$. For a discrete-time AR(1) process, the continuous-time analog is the Ornstein–Uhlenbeck process. Unfortunately, this results in an infinite number of zero crossings per unit length. While a continuous model is often a useful approximation to reality, in the case of zero crossings for a rough feature it ignores an important physical reality: the non-zero size of the molecules or atoms that make up the feature. If we consider Δy to be the smallest unit of material that can be added or removed from an edge, then it makes no sense to consider multiple zero crossings within the length Δy. Thus, the distance Δy will no longer be considered a sampling distance but instead will take on a physical meaning: the size of the atoms or molecules making up the feature. For the case of polymer-based photoresist, typical molecular size is on the order of $2 - 4$ nm.

From this zero-crossing result, we can derive an expression for η_a, the expected number of crossings of an arbitrary level a. Letting $f(x)$ be the probability of an edge or linewidth deviation of x,[8]

$$\eta_a = \eta_0 \left(\frac{f(a)}{f(0)} \right) \tag{8}$$

For a Gaussian probability distribution of roughness amplitudes, this gives for our AR(1) process

$$\eta_a = \eta_0 \, e^{-a^2/2\sigma^2} \approx \frac{L}{\pi} \sqrt{\frac{2}{\Delta y \xi}} \, e^{-a^2/2\sigma^2} \tag{9}$$

As an example, if $a = 3\sigma$, then there will be a factor of 90 fewer crossings at this level than zero crossings.

3. Comparison to Simulation

The number of zero crossings and certain non-zero level crossings, as predicted by equations (6) – (9), were checked against simulations using MetroLER v1.0 (Fractilia, LLC). A method for generating randomly rough features with a given power spectral density behavior has been previously described.[9] This method was used to simulate rough features, creating instantiations of a zero-mean random variable that could be interpreted as a rough feature edge. Then the zero crossings were counted for lines of varying length, sampling distance, and correlation length (keeping the roughness exponent fixed at 0.5). Typically 10^6 simulations were run and the results averaged to obtain the expected number of zero and level crossings.

The match between the exact equation (5) and the simulations were within simulation noise over a wide range of parameters. For example, a simulated line with 512 points has a standard deviation of zero crossings of $\sqrt{N}/2 = 11.3$. Running 10^6 simulations reduces this uncertainty by a factor of 1000, to 0.01 zero crossings for the feature. With $\Delta y = 1$ nm and $\xi = 10$ nm, the expected number of zero crossings for this line, according to equation (5), is 71.54. The average of 10^6 simulations produced 71.50 zero crossings (using a sub-sampling rate of 256 to approximate a continuous feature, i.e., 256 points along the rough line were generated per Δy interval). As the sub-sampling rate was varied from 1 to 256, the results clearly converged toward the 71.54 theoretical value (Figure 2), with the error inversely proportional to the number of subsamples.

Equation (8) or (9) can also be compared to simulation. For $a = 3\sigma$, a Gaussian distribution would result in a factor of 90.02 fewer level-a crossings than zero crossings. Figure 3 shows how the simulated ratio η_0/η_a approaches the ideal value when $\xi \gg \Delta y$.

For most purposes, the approximate expressions (7) and (9) can be used, which have errors of 1–3% for typical parameter settings. Thus, 10^4 simulations with $N = 512$ and using a sub-sampling rate of 32 will prove adequate for estimating the expected level-crossing rate, since this results in simulation errors typically less than 0.5%.
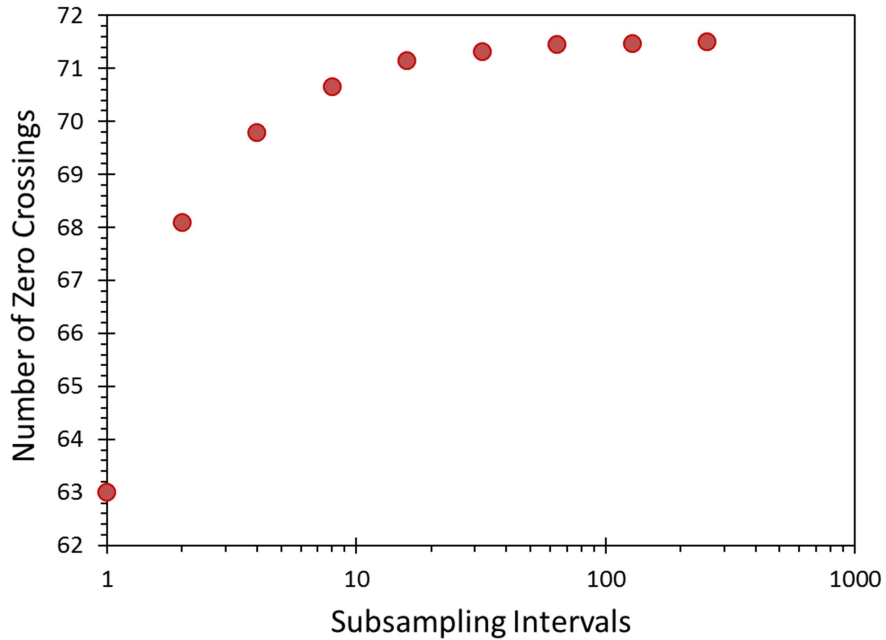
Figure 2.   Impact of sub-sampling rate (the number of points generated for the rough feature within one interval Δy) on the simulated number of zero crossings ($N = 512$, $\Delta y = 1$ nm, $\xi = 10$ nm, $H = 0.5$). The simulation values converge to the theoretical value of 71.54 as the sub-sampling rate increases.
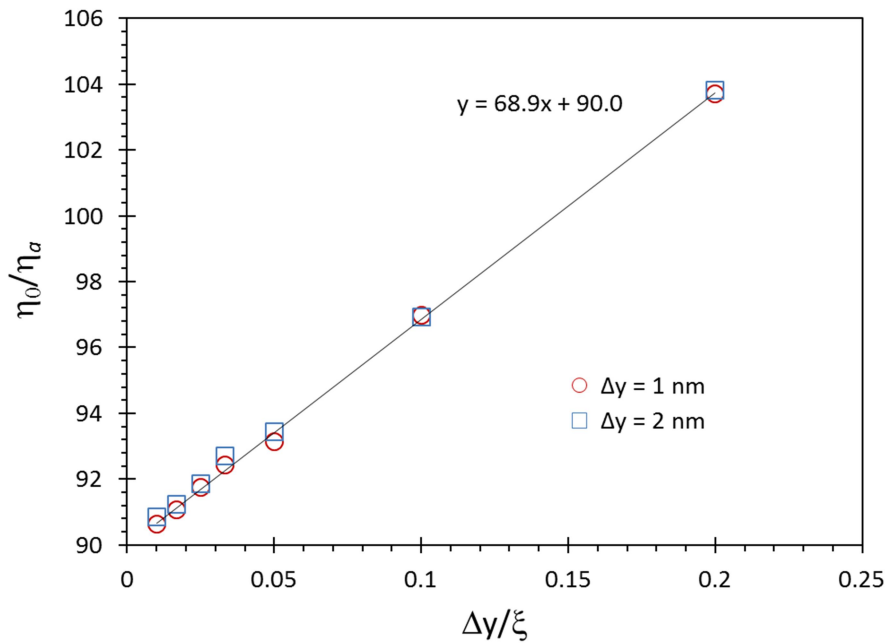

Figure 3.   Impact of correlation length on the ratio of the expected number of zero crossings to the expected number of 3σ level crossings ($N = 2048$, $\Delta y = 1$ or 2nm, ξ varied, subsampling rate of 32, 10^6 simulations per data point, $H = 0.5$).

Simulation can now be used to explore the impact of the roughness exponent H on the expected number of zero crossings. The frequency distribution of the roughness will have a strong impact on the number of zero crossings. A sine wave will produce two crossings per cycle, so that the high frequency components of roughness will produce more zero crossings than the low frequency components. The impact of higher H is to increase the downward slope of the PSD in the high-frequency region (see equation (1)), thus suppressing high-frequency roughness. One would expect, then, that increasing the roughness exponent will decrease the expected number of zero crossings, all other things kept equal. Figure 4 shows that this indeed is the case. Further, the ratio η_0/η_a does not change more than a few percent over this range of parameters.
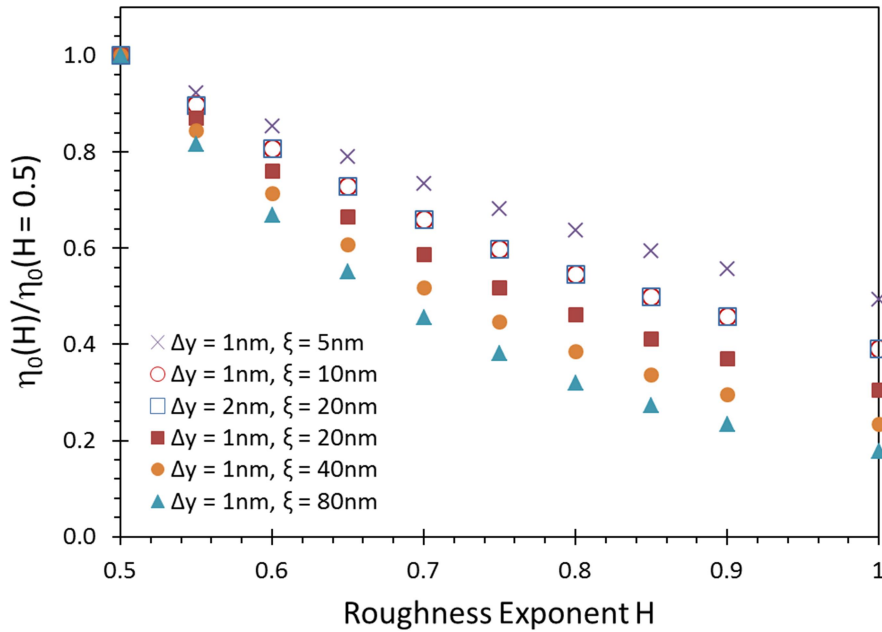

Figure 4.   Impact of roughness exponent on the expected number of zero crossings ($N = 512$, subsampling rate of 32, 10^6 simulations per data point).

An approximate expression that matches these simulation results is

$$\eta_0(H) \approx \eta_0(H = 0.5)\left(\frac{\Delta y}{\xi}\right)^{\ln(H+0.5)} \tag{10}$$

To see how well this model equation works, the same simulated data from Figure 4 is plotted against the predictions of equation (10) in Figure 5. The relative error between equation and simulation is less than 5% over this range of conditions.
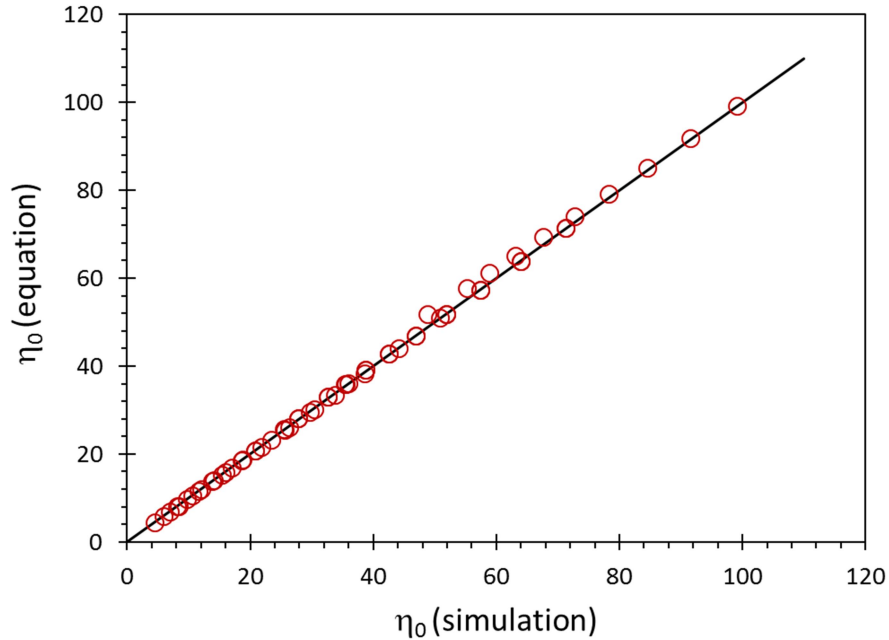
Figure 5.   Comparison of the simulated number of zero crossings to predictions made by equation (10) ($N = 512$, subsampling rate of 32, 10^6 simulations per data point, with other parameters as shown in Figure 4).

An interesting and important property of the zero-crossing rate (the number of zero crossings per unit length) is that it is independent of the amount of roughness (σ). Thus, it provides a method of separately measuring correlation length and roughness exponent independent of σ. With that idea in mind, we will now look at how to measure the number of zero crossings of a rough feature, and how measurement biases and errors will impact it.

4.   Impact of Metrology on the Measured Level Crossings

The simulations described above were ideal in the sense that they describe the actual behavior of a simulated rough line. In that application, Δy represents the molecular size of the feature material. Simulations can also be used to understand the real-world effects of measurement. When measuring the number of level crossings, one must use a metrology tool that does not describe the exact edge position or linewidth, but rather has a number of non-ideal aspects. For example, all measurements include metrology noise, essentially white noise spread evenly across all frequencies. Further, all measurement tools have a nonzero measurement probe width that averages the edge position over that probe width, smoothing out the very high frequency roughness. Additionally, while the simulations above created zero-mean random variables, experimental measurement involves detrending: subtracting off the sample mean for LWR measurement and a best-fit line for LER measurement. Simulation can be used to understand the impact of each of these metrology effects.

When simulating the measurement of the number of level crossings, Δy takes on the common metrology meaning: the spacing between measurement points along the feature. First, consider the impact of metrology averaging due to a nonzero metrology probe width. If the metrology probe has a Gaussian shape (due to a nonzero beam spot size plus electron scattering within the sample, for example), then the full-width half-maximum (FWHM) size of the probe will determine the amount of averaging. Figure 6 depicts

the number of zero crossings relative to an ideal zero-width measurement probe. The correlation length has no impact on the metrology probe averaging effect, but the roughness exponent does. For probe widths near or less than the measurement grid spacing Δy, the decrease in the measured number of zero crossings is approximately given by

$$\eta_0(pw) \approx \eta_0(pw=0)\left[1-(0.4-0.3H)\frac{pw}{\Delta y}\right] \tag{11}$$

where pw = the FHWM Gaussian probe width.

Metrology probe averaging reduces the observed number of 3σ level crossings to an even greater extent. As a result, the observed ratio of zero to 3σ level crossings increases with more metrology probe averaging, as described by this empirical expression:

$$\frac{\eta_0}{\eta_a} \approx 90\left[1+\frac{0.5}{H^2}\left(\frac{pw}{\xi}\right)\right] \tag{12}$$

While the metrology probe width averages high-frequency roughness and reduces the number of observed zero crossings, metrology noise has the effect of adding back high frequency roughness and increasing the number of observed zero crossings (Figure 7). Letting σ_{MN} be the metrology noise, the number of zero crossings will increase approximately as
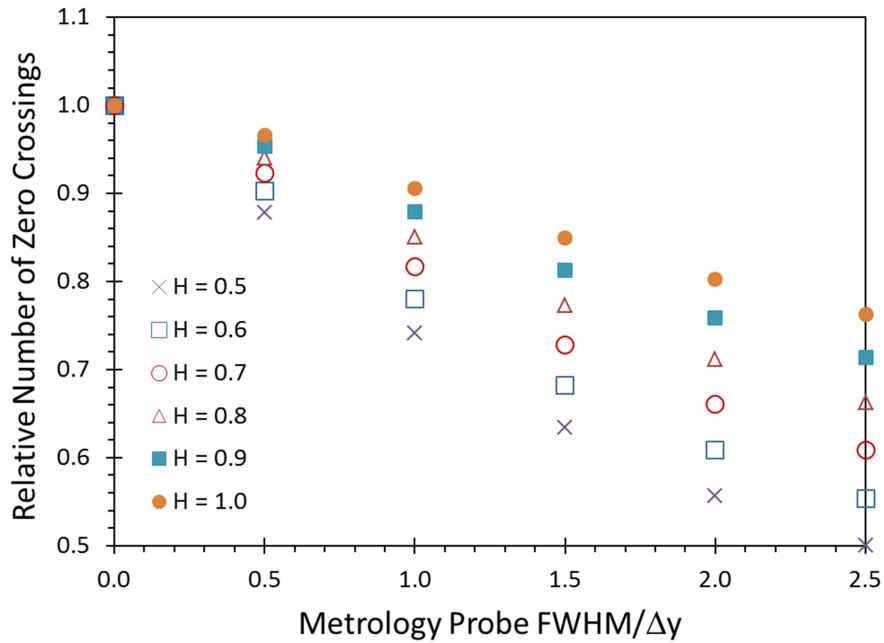
$$\eta_0(\sigma_{MN}) \approx \eta_0(\sigma_{MN}=0)\left[1+(2H-0.6)\left(\frac{\xi}{\Delta y}\right)\left(\frac{\sigma_{MN}}{\sigma}\right)^{1.5}\right] \tag{13}$$

The number of 3σ level crossings grows even faster with added metrology noise. As a result, the observed ratio of zero to 3σ level crossings decreases with more metrology noise. This ratio is approximately independent of Δy, ξ, and H.

$$\frac{\eta_0}{\eta_a} \approx 90\left[1-\left(\frac{\sigma_{MN}}{\sigma}\right)\right] \tag{14}$$
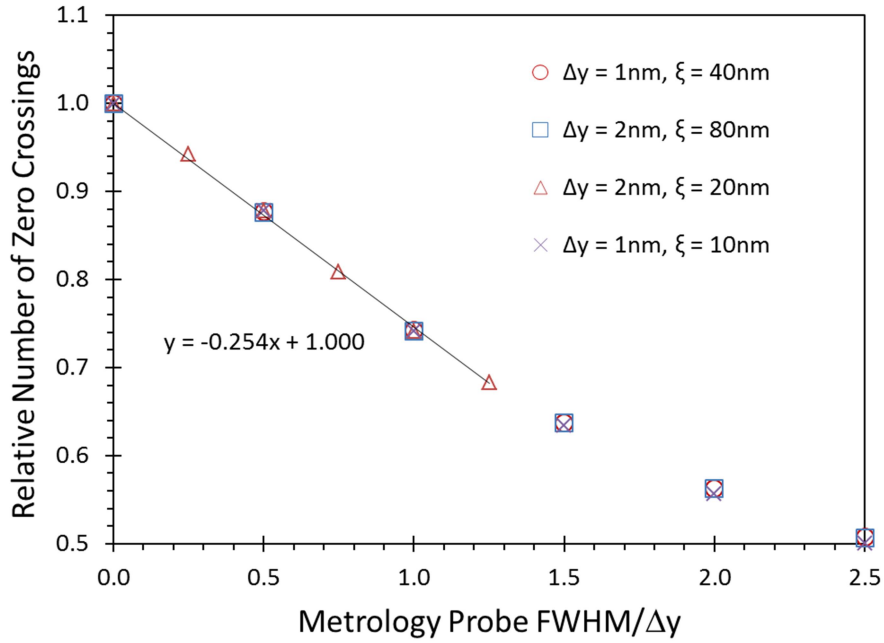
(a)

(b)

Figure 6.   Impact of metrology probe width on the measured number of zero crossings ($N = 512$, subsampling rate of 32, 10^6 simulations per point):   (a) $H = 0.5$ and varying correlation lengths and measurement increments; (b) $\xi/\Delta y = 10$ and varying H.
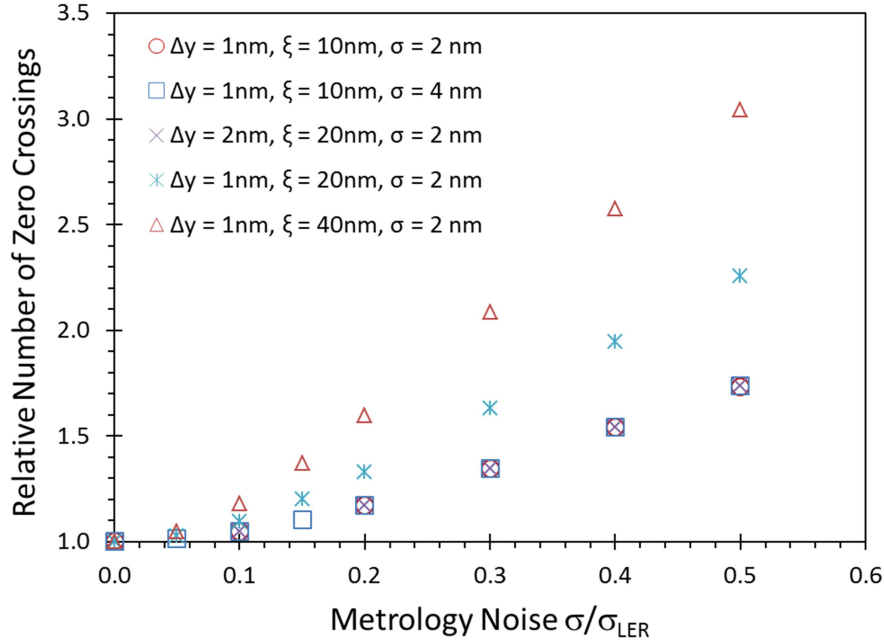
Figure 7. Impact of metrology noise on the measured number of zero crossings ($N = 512$, $H = 0.5$, subsampling rate of 32, 10^6 simulations).

As is also true of PSD measurement[10,11] and height-height correlation measurement,[12] it is possible for metrology averaging and metrology noise to cancel out, depending on the parameters of the process and the metrology. For $H = 0.5$, this occurs approximately when

$$pw \approx 1.6 \Delta y \left(\frac{\sigma_{MN}}{\sigma} \right)^{1.5} \qquad (15)$$

For example, if the metrology noise is 25% of the LER, then noise and probe averaging cancel when the probe width is 20% of the sampling distance. If $\sigma_{MN} = 0.75\sigma$ (a high but not uncommon level of noise), then the two effects cancel with pw equal to the sampling distance.

Detrending is also a reality of measuring roughness. To calculate the LWR, we substrate off the sample mean (the average linewidth). To calculate the LER, we find the deviation of the feature edge to its best-fit straight line. But detrending also removes low-frequency roughness from the data. By simulating rough features and counting the zero and level crossings with and without the detrending of a single feature or edge, the following empirical expressions match the observations:

$$\eta_{0-mean} \approx \eta_0 \left[1 + \frac{\xi}{L} \right] \qquad (16)$$

$$\eta_{0-linear} \approx \eta_0 \left[1 + \frac{2\xi}{L} \right] \qquad (17)$$

$$\eta_{a-mean} \approx \eta_a \left[1 - \frac{8\xi}{L} \left(1 - \frac{3\xi}{L} \right) \right] \tag{18}$$

$$\eta_{a-linear} \approx \eta_a \left[1 - \frac{16\xi}{L} \left(1 - \frac{3\xi}{L} \right)^2 \right] \tag{19}$$

Thus, the impact of detrending becomes small when $L \gg \xi$.

Based on these simulations, we propose the measurement of the number of zero crossings and the number of 3σ level crossings as a useful tool for characterizing LER and LWR. Such measurements can supplement the more common PSD or HHCF analysis.

5. Comparison to Experimental Data

Experimental level-crossing results were obtained from SEM images of EUV lithography samples exposed using an IBM process.[13] Using the ASML NXE:3300 scanner, 18-nm half-pitch patterns were printed in a polymer-based chemically amplified resist and then imaged on a Hitachi CG-5000 CD-SEM (512x512 pixels per image, x-pixel size = 0.88 nm, y-pixel size = 5.00 nm). Edge detection was performed using the Analytical Linescan Model (ALM) algorithm of MetroLER with no image filtering and a threshold of 0.5.[14] Figure 8 illustrates one result. Even with an extremely noisy SEM image, accurate edge detection is possible with the ALM without the modifying effects of image filtering. Thirty images were collected and the analysis results from each of the measured features were combined.

Analysis of the power spectral density and height-height covariance functions produced a (biased) LER 1-sigma value of 1.22 nm (standard error = 0.002 nm based on the 720 edges measured) and an estimated correlation length of 7.2 nm (standard error = 0.12 nm). Level crossings were measured in both the positive direction (edge deviations in a direction that make the resist line wider) and the negative direction (edge deviations in a direction that make the resist line narrower). Results are shown in Tables I and II.
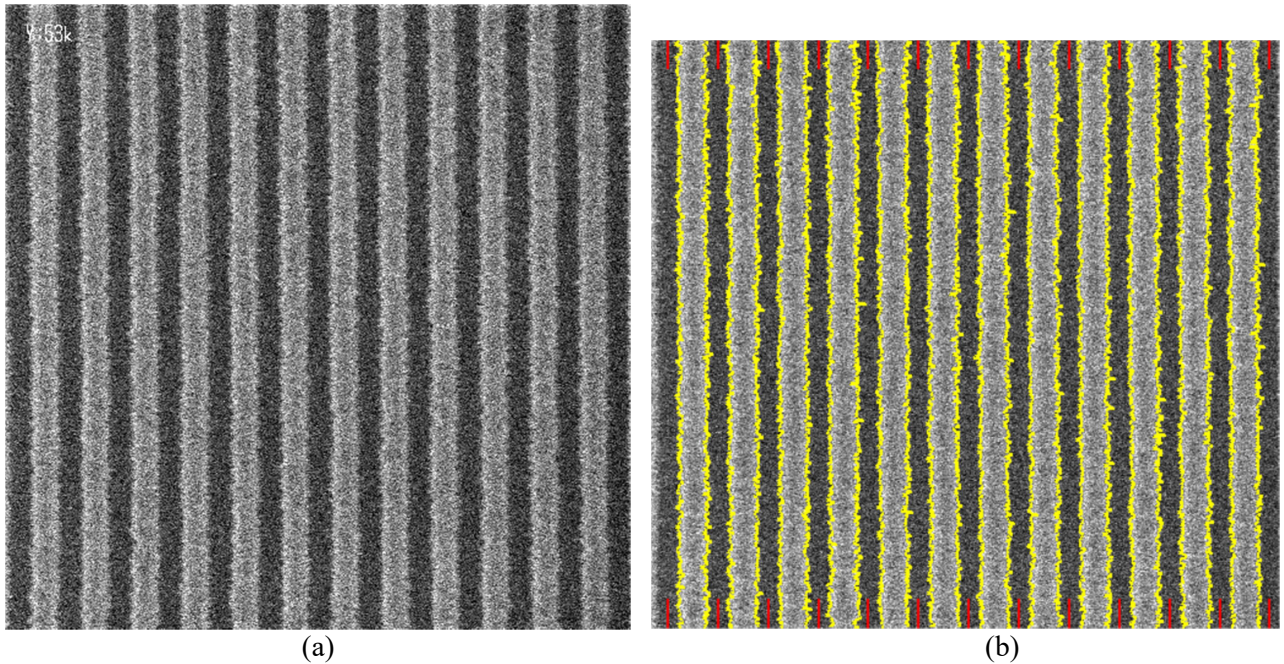
<div align="center">(a)   (b)</div>

Figure 8.　An example SEM image of an EUV exposure of 18 nm lines and spaces: (a) original image, and (b) after edge detection using the ALM (analytical linescan model) with a threshold of 0.5.

Table I. Measured level crossings for both left and right edges of 30 images (12 lines per image) with L = 2400 nm and Δy = 5 nm.   Left LER 1-sigma = 1.10 nm and right LER 1-sigma = 1.28 nm.

Level Crossings per Edge	Positive	Negative
zero crossings	189.2	189.2
1-sigma crossings	102.8	105.4
2-sigma crossings	20.1	22.4
3-sigma crossings	2.10	3.03
4-sigma crossings	0.19	0.43

Table II. Mean distance between crossings measured for 30 images (12 lines per image) with L = 2400 nm and Δy = 5 nm. Expected values assume Gaussian statistics, LER 1-sigma = 1.19 nm, and correlation length = 7.2 nm.

Mean Distance Between (nm)	Positive	Negative	Expected
zero crossings	12.7	12.7	15.0
1-sigma crossings	23.4	22.8	24.7
2-sigma crossings	120	108	111
3-sigma crossings	1140	794	1350
4-sigma crossings	12,400	5,600	44,700

As seen in Table II, expected results follow closely the measured mean distance between crossings for the cases of zero crossings, 1-sigma crossings, and 2-sigma crossings. For the 3-sigma crossings, the distance between crossings is about 15% less than expected assuming constant Gaussian statistics for the

case of positive crossings, and about 40% lower for negative crossings (nearly twice as many negative level crossings as expected). At the 4-sigma level, there were about 4 times more crossings detected than expected for positive crossings, and 8 times more crossings for negative crossings (about 140 positive crossings and 310 negative crossings in total). This far higher than expected number of 4-sigma crossings does not bode well for the possibility of catastrophic line failure and begs for an explanation.

The metrology simulations discussed above may offer some insight. Metrology noise increases the number of zero crossings, while metrology averaging decreases it. Since the measured number of zero crossings closely matches the expected number, it seems that these two metrology biases are approximately canceling out. For this data, the metrology noise σ_{MN} was estimated to be 0.8 nm for the left edge and 1.0 nm for the right edge. Also, a typical value for the metrology averaging is on the order of $pw = 5 - 8$ nm. Using equations (11) and (13) we estimate that metrology noise should increase the expect number of zero crossings by about 40%, while metrology averaging would decrease them by about 30%. For the case of 4-sigma crossings, simulations showed about 1.6X more level crossings than expected under these noise and averaging conditions for the left edge, and 1.8X more level crossings for the right. Thus, some of the observed increase measured level crossings compared to expectations can be attributed to metrology noise. But there remains an unexplained higher than expected number of 4-sigma crossings which indicates that the assumption of a purely Gaussian distribution of edge errors is likely to be at fault.

Normal probability plots (or, in general, Q-Q plots) are commonly used to check an assumption of normality. Figure 9 shows examples of normal probability plots for one measured SEM image. Left and right edges produce somewhat different results due to the asymmetry of the linescan in the scan direction.[15] The results indicate normal (Gaussian) behavior out to about ±2.5 nm of edge deviation (corresponding to about 2-sigma LER). Beyond, this, the tails of the distribution are heavier than Gaussian.
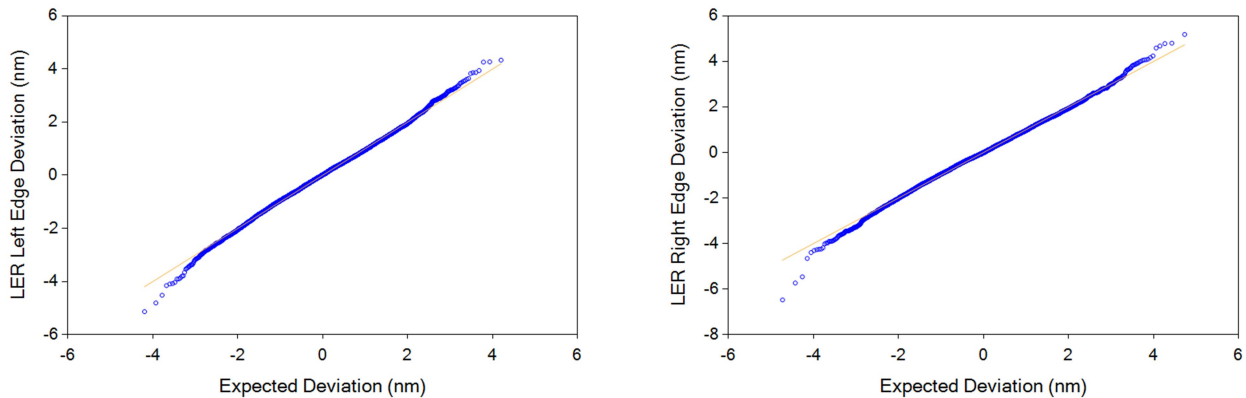

Figure 9.   Normal probability plots showing the edge deviations of the left and right edges for all the features in one SEM image (the image shown in Figure 8). The straight line indicates perfectly Gaussian behavior.

In hindsight, such heavy tails are to be expected. A simple model of edge roughness predicts that noise in the final edge position is the ratio of noise in the energy deposited in the resist at the line edge divided by the energy gradient at the line edge. For a sinusoidal exposure dose profile (appropriate for dense lines and spaces assuming two-beam imaging), the energy gradient (image slope) is maximal at the half-pitch edge position, then falls off approximately quadratically as the line edge deviates from this position. This decrease in energy gradient should cause an increase in edge position variation for the same level of energy noise. Further, the relative noise in the image is proportional to one over the square root of the image

intensity, which means there will be less image noise in the space due to the higher intensity there. Thus, if the edge deviations are Gaussian distributed near the nominal half-pitch line position, edge deviations farther away will occur more frequently (i.e., have heavier tails) due to the lower energy gradient, and negative edge deviations will occur more frequently than positive deviations do to the lower number of photons in the negative edge direction.

The data in Figure 9 can be fit to a heavy-tailed distribution rather than a Gaussian distribution. While the experimental distribution is not symmetrical, the Student's t-distribution will be used here as a simple example of a heavy-tailed distribution. The data from Figure 9 is well fit to a Student's t-distribution when the degrees of freedom (DF) is about 13 for the right edge and about 20 for the left edge when moving in the worst direction. The significance of the heavy tails is clear when extrapolations are required (that is, to predict when a bridge or break in a line might occur). For a Student's t-distribution, the equivalent of equation (9) is obtained from

$$\eta_a = \eta_0 \left(1 + \frac{(a/\sigma)^2}{DF} \right)^{-\left(\frac{DF+1}{2} \right)} \tag{20}$$

Using the data from Tables I and II as an example, a level of $a = 9\sigma$ corresponds to an edge error of about 11 nm (probably catastrophic for these 18 nm features). For a molecular size of 2 nm, we can predict the zero-crossing rate to be $\eta_0/L \approx 0.11$ nm^{-1}. If the edge deviation distribution were Gaussian, we would expect $\eta_a = 1$ (one catastrophic failure on average) when the line length is 3×10^9 m, so that a catastrophic failure would be highly unlikely in any given chip. However, if the Student's t-distribution with DF = 15 applied, the mean line length between failures would be 0.02 m, almost guaranteeing that every chip would fail. Obviously our ability to extrapolate out to $a = 9\sigma$ depends greatly on the assumed distribution of edge errors.

One important caveat is in order. The experimental evidence presented in Tables I and II depends on the accuracy of the edge detection used on the SEM images. These SEM images proved exceedingly noisy, so that reliable edge detection was difficult. Techniques that filter the SEM image in order to reliably detect edges will necessarily smooth away some roughness, changing the zero and level crossing results, and making extrapolation impossible. But failed edge detection will result in extreme edge values, thus inflating the counts of 4-sigma and 5-sigma level crossings. Here, the Analytical Linescan Model was used to provide robust and accurate edge detection. However, any sufficiently noisy linescan will cause even that edge detection algorithm to fail as well. Thus, careful attention should be paid to the noise level in the SEM images and the robustness of the edge detection algorithm when making level crossing measurements.

6. Conclusions

Here, a new methodology for characterizing stochastic-induced roughness in lithography has been introduced: the level crossing method. This method uses edges detected from a standard SEM image to count the number of times each edge crosses a certain level (distance away from its mean position). Among other uses, this technique allows an independent approach to extracting correlation length by measuring the number of zero crossings, especially if the sampling distance Δy can be varied. Further, counting the level crossings for different levels (for example, 1σ, 2σ, 3σ, etc.) allows an assessment of the probability distribution of edge deviations.

While further effort is required, the preliminary results presented here indicate that edge deviations have much heavier tails than a Gaussian distribution. For example, the number of 4-sigma crossings was found to be 6.6 times higher than expected under the assumption of a Gaussian distribution. Since extrapolation of any measured probability distribution into unmeasured regions of extreme values must necessarily be risky, further efforts at modeling roughness variation using the positional dependence of the image slope might prove fruitful. If the image log-slope as a function of position is known, and the standard deviation of roughness is inversely proportional to the image log-slope, it may be possible to predict the non-Gaussian tails of the observed distribution and more accurately extrapolate to rare events.[3] Additionally, the measurement of level crossings necessarily employs "biased" edges, that is, edges that include metrology noise such as SEM image noise. How this noise might be corrected for is still an open research question.

References

[1] Chris A. Mack, "Analytical Expression for Impact of Linewidth Roughness on Critical Dimension Uniformity", *Journal of Micro/Nanolithography, MEMS, and MOEMS*, **13**(2), 020501, (2014).

[2] Chris A. Mack, "Understanding the efficacy of linewidth roughness post-processing", *Journal of Micro/Nanolithography, MEMS, and MOEMS*, **14**(3), 033503 (2015).

[3] Timothy A. Brunner, Xuemei Chen, Allen Gabor, Craig Higgins, Lei Sun, and Chris A. Mack, "Line Edge Roughness (LER) performance targets for EUV Lithography", *Extreme Ultraviolet (EUV) Lithography VIII*, SPIE Vol. 10143 (2017).

[4] S. O. Rice, "Mathematical Analysis of Random Noise", reprinted in *Noise and Stochastic Processes*, Nelson Wax, Ed., Dover (1954).

[5] G. Palasantzas, "Roughness spectrum and surface width of self-affine fractal surfaces via the K-correlation model", *Phys. Rev. B*, **48**(19), 14472-14478 (1993).

[6] Benjamin Kedem, *Binary Time Series*, Marcel Decker, New York, 45-50 (1980).

[7] Benjamin Kedem, "Spectral Analysis and Discrimination by Zero-Crossings", *Proc. IEEE*, **74**(11), 1477-1493 (1986).

[8] Athanasios Papoulis, *Probability, Random Variables, and Stochastic Processes*, McGraw-Hill, New York, 345-350 (1984).

[9] Chris A. Mack, "Generating random rough edges, surfaces, and volumes", *Applied Optics*, **52**(7), 1472-1480 (2013).

[10] Chris A. Mack, "Systematic Errors in the Measurement of Power Spectral Density", *J. Micro/Nanolith. MEMS MOEMS*, **12**(3), 033016 (Jul-Sep, 2013).

[11] Chris A. Mack, "More systematic errors in the measurement of power spectral density", *Journal of Micro/Nanolithography, MEMS, and MOEMS*, **14**(3), 033502 (2015).

[12] Chris A. Mack, "Biases and uncertainties in the use of autocovariance and height-height covariance functions to characterize roughness", *Journal of Vacuum Science & Technology B*, **34**(6), 06K701 (2016).

[13] Nicole Saulnier, et al., "EUV processing and characterization for BEOL", Proc. SPIE 9422, 94220T (2015).

[14] Chris A. Mack and Benjamin D. Bunday, "Analytical Linescan Model for SEM Metrology", *these proceedings*, *Metrology, Inspection, and Process Control for Microlithography XXXI*, (2017).

[15] Lei Sun, Nicole Saulnier, Genevieve Beique, Erik Verduijn, Wenhui Wang, et al., "Comparison of left and right side line edge roughness in lithography", Proc. SPIE 9778, *Metrology, Inspection, and Process Control for Microlithography XXX*, 977822 (2016).